

We are IntechOpen, the world's leading publisher of Open Access books Built by scientists, for scientists

6,900

Open access books available

186,000

International authors and editors

200M

Downloads

Our authors are among the

154

Countries delivered to

TOP 1%

most cited scientists

12.2%

Contributors from top 500 universities



WEB OF SCIENCE™

Selection of our books indexed in the Book Citation Index
in Web of Science™ Core Collection (BKCI)

Interested in publishing with us?
Contact book.department@intechopen.com

Numbers displayed above are based on latest data collected.
For more information visit www.intechopen.com



Multi-Level Mathematical Modeling of Solid Oxide Fuel Cells

Jakub Kupecki, Janusz Jewulski and
Jarosław Milewski

Additional information is available at the end of the chapter

<http://dx.doi.org/10.5772/50724>

1. Introduction

In recent years, numbers of questions concerning energy generation have arisen. Emission levels, delivery security, and diversification of the portfolio of technologies have been extensively discussed. Well-established generation based on fossil fuels in large-scale power stations is criticized for big environmental impacts, and limited sustainability due to high fraction of process losses. Not only emissions, but also extraction of resources, alternation of the landscape, transmission and distribution inefficiencies are often pointed as the main downside. As a solution for rapidly increasing energy consumption, and emerging threat of current resources depletion, distributed generation based on highly efficient micro- and small-system was proposed. Moreover, combined heat and power (CHP) units with high achievable efficiency are seen as possible substitutes for stand-alone electricity generators. Most of technologies from that group are currently under development, however selected systems are already reaching market availability. In 2004 European Commission indicated selected systems, with guidelines for promotion and development of highly efficient co-generative units [1]. List of technologies, which can provide high electrical and overall efficiency with limited environmental impacts, includes the following:

- Combined cycle gas turbine with heat recovery
- Steam backpressure turbines
- Steam condensing extraction turbines
- Gas turbines with heat recovery

- Internal combustion engines
- Microturbines
- Stirling engines
- Fuel cells
- Steam engines
- Organic Rankine cycles
- Any other type of technology or combination of thereof falling under the definition laid in the directive

Further studies were devoted to finding the optimal technology for micro- and small scale-systems suitable for CHP applications. It should be noted that, to distinguish between selected systems scales, terms micro and small were introduced. In the EU Combined Heat and Power directive [1] the earlier term refers to units with nominal power output 50 kW_{el} while in literature it usually covers systems with nominal power output of single kW_{el} [2,3,4]. The later usually refers to system with output of tens of kW_{el} .

It was found that three groups of technologies are especially interesting from the technical and economical point of view for systems with single kilowatts power output, namely:

- Internal combustion engines
- Stirling engines
- Fuel Cells (PEFC and SOFC)

While different energy generating systems with internal combustion and Stirling engines are a well-established technology, fuel cells in stationary generation have been known for not more than two decades. Even though technology is not yet mature, numerous demonstration systems have already been operated allowing to gain operating experience. The main reason to consider fuel cells as an alternative to other generation systems is high electrical performance due to the direct conversion of chemical energy of a fuel into electricity.

Evaluation of PEFC and SOFC for micro-CHP application was recently presented [3]. Authors underlined high efficiency and multifuel capabilities of the SOFC. Additionally, in case of low-temperature cells, such as PEFC, partial internal reforming cannot be done, hence efficiency penalty due to external reforming is observed next to limited fuel flexibility. Moreover, SOFCs offer utilization of high temperature heat in co-generative systems [4]. Substantial part of the high-grade heat can be recovered from the anodic and cathodic gas streams leaving the SOFC stack at elevated temperature [5] for hot tap water supply or heating purposes [6]. Taking into account these advantages, SOFC technology has been selected for further analysis with different modeling techniques.

2. Selected systems with Solid Oxide Fuel Cells

Over the years fuel cell technology proved to be feasible in a number of applications, including portable energy generation, transportation, stationary back-up systems and energy generators in space missions among others. Currently, selected fuel cells such as SOFCs are considered as suitable conversion systems for the clean and sustainable energy generation. Development of such systems requires proper modeling approaches, construction of high fidelity numerical simulators and tools able to provide clear insight into various aspects of the system operation.

Selected units with SOFCs have already reached proof-of-the-concept stage of development, and in some cases units are already available in for sale. Comparison of market-available systems is presented in Table 1, based on available data [7,8,9,10,11,12,13]. It should be emphasized, that using fuel cells for electricity only generation in micro- and small-units is not economically feasible, therefore it was not considered. SOFC-based electricity-only generation is economically feasible only for the capacity range over 100 kW_{el}. For such systems expected electrical efficiency ranges between 40 and 85%, while capital and operation and maintenance (O&M) costs were estimated for 1500-3000 \$/kW and 0.0019 – 0.0153 \$/kW, respectively [14]. By comparing these numbers with data for other systems presented in Table 2 it becomes clear that SOFC can be indeed competitive.

Vendor	Type of fuel cell	Power: electrical/thermal [kW]	Efficiency: η_{el}/η_{tot} [%]	Number of units
Hexis	SOFC	1.0/2.0	30-35/>90	42
CFCL	SOFC	1.5/0.6	60/85	>10
Vaillant	SOFC	4.6/6.5	30/88	>60
JX Nippon	SOFC	0.7/1.25	45/87	800
Baxi	PEFC	1.0/1.7	32/85	>20
Viessmann	PEFC	2.0/5.0	28/80	10
Bosch	PEFC	4.6/6.5	29/80	10

Table 1. Comparison of selected micro-CHP systems with fuel cells.

Different concepts of large SOFC-based systems were developed and studied [15,16,17]. Among those, various plants proposed by Siemens-Westinghouse with nominal power ranging from single up to hundreds MW_{el} were investigated [18,19], including pressurized systems. Despite the fact that high efficiency and near-zero emissions in such plants were envisioned, attention has been focused on smaller scales – single and tens of kW_{el}.

Technology	Capacity	η_{el} [%]	Capital cost [\$ /kW]	O&M costs [\$ /kW]
Disel engines	500 kW - 50MW	35	200-350	0.005 - 0.015
Gas turbines	500 - 5 MW	29 - 42	450 - 870	0.005 - 0.0065
Photovoltaic system	1 kW - 1MW	6 - 19	6600	0.001 - 0.004
Wind turbines	10 kW - 2MW	25	1000	0.01

Table 2. Comparison of selected systems for stand-alone electricity generation.

3. Modeling: transition between different length and time scales

During SOFC-based system operation numbers of different processes are taking place at different length- and time-scales. Summary of typically considered phenomena is presented in Table 3.

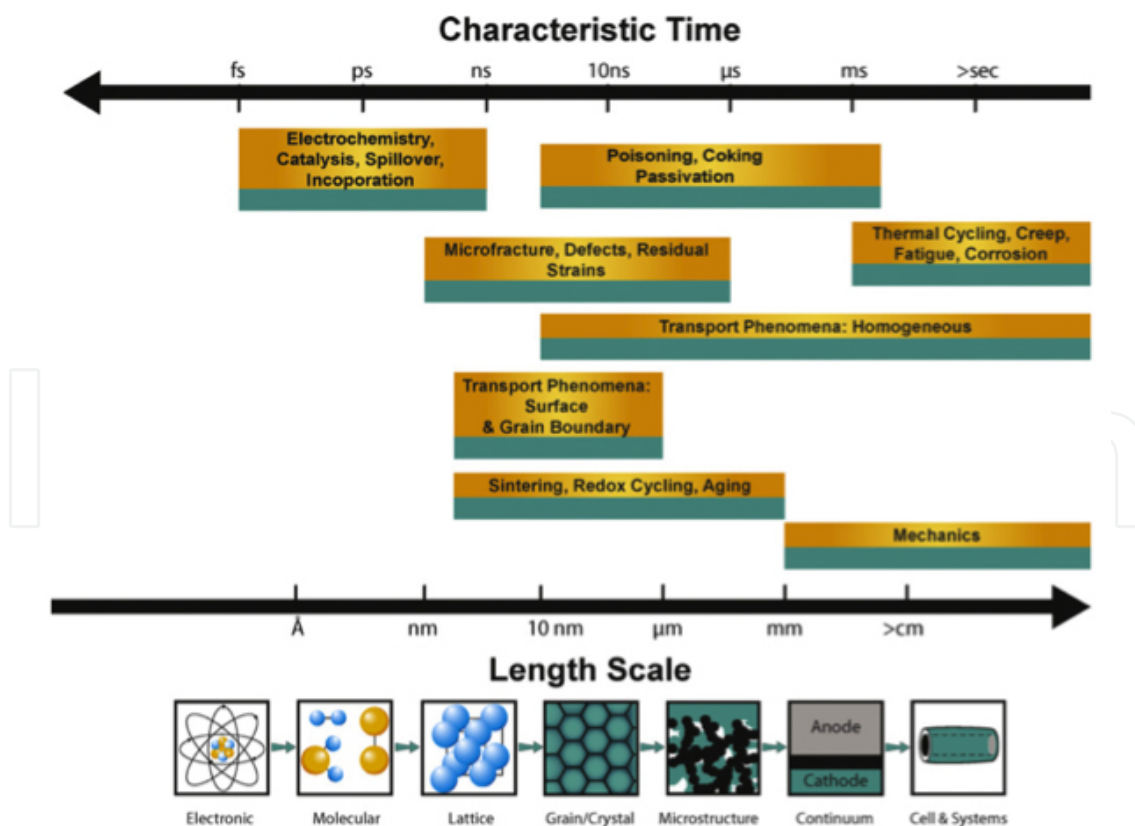


Figure 1. Different processes and their corresponding length scales and time frames (after [20])

Scale [m]	Structure	Phenomena
10^{-8} – 10^{-7}	Electrode material Triple phase boundary – electrode, electrolyte and oxidant contact point	Electrochemistry Diffusion through the surface Chemical reaction
10^{-7} – 10^{-5}	Porous media	Knudsen diffusion Flow through porous media Chemical reaction
10^{-5} – 10^{-3}	Flow field	Diffusion Mass flow Heat exchange
10^{-3} – 10^{-2}	Single cell	Transport of oxidant and fuel Thermal balancing
10^{-2} – 10^0	Stack	Electrical circuits of the cell Processes in the electrical system Thermal balancing
10^0 – 10^7	System level	Control, automatics, safety systems Integration of the entire system

Table 3. Selected processes taking place during SOFC-system operation and their corresponding length scales.

Application-specific criteria and various designs require dedicated methodology for detailed investigation of processes listed in Table 3. In general, models are used to help understand and predict behavior of a particular system, to optimize control strategy, thermal balancing, and other aspects. Additionally, optimization tools can provide information on the optimal operational parameters. Moreover, models can be used as predictive tools for performance evaluation under off-design conditions. Modeling can provide crucial information for the system configuration improvements. Work on a prototype design is usually an iterative procedure where modeling is coupled with design definition. In each case, determination of criteria is an important step and must correspond to particular requirements. Depending on type of modeling, desired complexity and level of details, sufficient data have to be supplied to model. This section will briefly review different modeling techniques, including 0, 1-2 and 3D models. In a recent and valuable summary of modeling and simulation techniques [20] pictorial illustration of different issues and their corresponding length scales (Table 3) and characteristic time has been proposed (Fig. 1).

Models can be divided into macro- and micro-scale, depending on the length scales that are covered by particular approach. In general case, analysis of SOFC at the stack level focuses

on development of models for electrochemical processes, chemical reaction, transport phenomena, and geometry influence. Investigation of the entire system includes studies on the integration, heat and mass exchange, electrical circuits, and equipment.

3.1. 0D modeling

Zero-dimensional methodology allows studying processes that can be analyzed without taking into account spatial configuration and geometry. Such approach is justified for system-level studies, however might also be used for estimation of certain parameters. Depending on the required precision, 0D models can be used to solve governing equations for planar SOFC, written for each of the cell components: electrodes, electrolyte, interconnects and flow channels [21,22,23,24,25]. Required assumptions include constant fluid properties, air as an incompressible gas and no chemical reactions occurring in the fuel and air channels. Set of governing equations is later solved with desired accuracy by different algorithms. System-level studies can be performed with commercially available software such as Aspen Plus or Aspen Hysys. The later was recently used by Kupecki and Badyda [5] for evaluation of different fuel processing technologies for micro-CHP unit with SOFC. Different designs, presented in Fig. 2-6 were studied for evaluation of heat and mass balances. In the study, characteristics of market-available SOFCs were implemented, and auxiliary equipment was selected for off-the-shelf products. Considering different fuels, including natural gas, diesel, and LPG it was possible to define the optimal processing technology for micro-CHP unit equipped with afterburner. Steam reforming allowed achieving the highest overall system efficiency, even though it required substantial amount of heat. Generally, 0D method proved to be sufficient for system-level studied, including thermal processes (i.e. heat exchange, heat losses, combustion in the afterburner), electrochemical reactions in the SOFC stack and chemical reactions occurring in the fuel processor.

With introduction of heat capacity, dynamics can be studied to some extent using 0D modeling techniques, as it will be presented in the dynamic modeling section. In certain cases chemistry can also be investigated. The main limitation is the difficulty to explicitly incorporate geometry of chemical reactors, although semi-empirical correlations are sometimes applicable. Bove and Ubertini [26] suggested using black-box 0D models to investigate impact of fuel composition, oxidant or fuel utilization and overpotentials on the macroscopic performance of SOFC in terms of efficiency and current-voltage characteristics. Such models should be used when system-level approach is required, without main focus on the SOFC stack itself [27]. In cell-leveling modeling, zero dimensional approach can be efficiently used for solving elementary balance equations for fluids: continuity, momentum, energy and species transport. Since solid oxide fuel cells consists of two porous electrodes separated by an electrolyte, porosity of these materials should be explicitly considered in the governing equations. Once the set of equations is developed, it can easily be transferred from discrete 0D to 1D model to be solved using proper CFD method [28].

Summarizing, the main advantage of zero-dimensional approach is low computational costs, simple formulation of the model. Such models can be freely used for systems where

no mass and heat accumulation occurs. The main disadvantage is the significant limitation in modeling influence of geometry and sizing, especially when those are of a high importance, for instance in chemistry modeling.

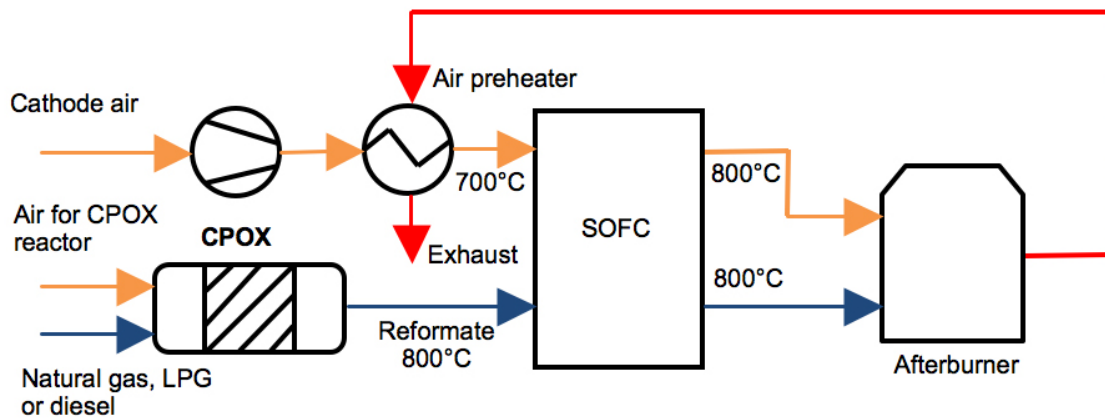


Figure 2. Single-pass system with CPOX reactor

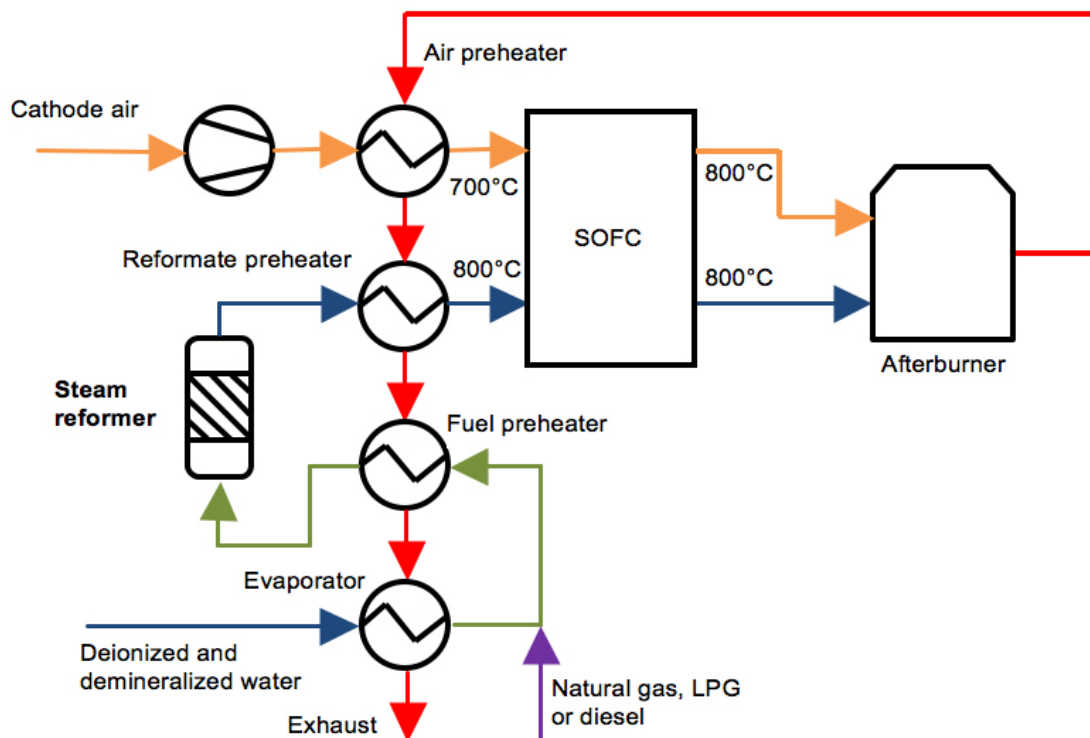


Figure 3. Single-pass system with steam reformer

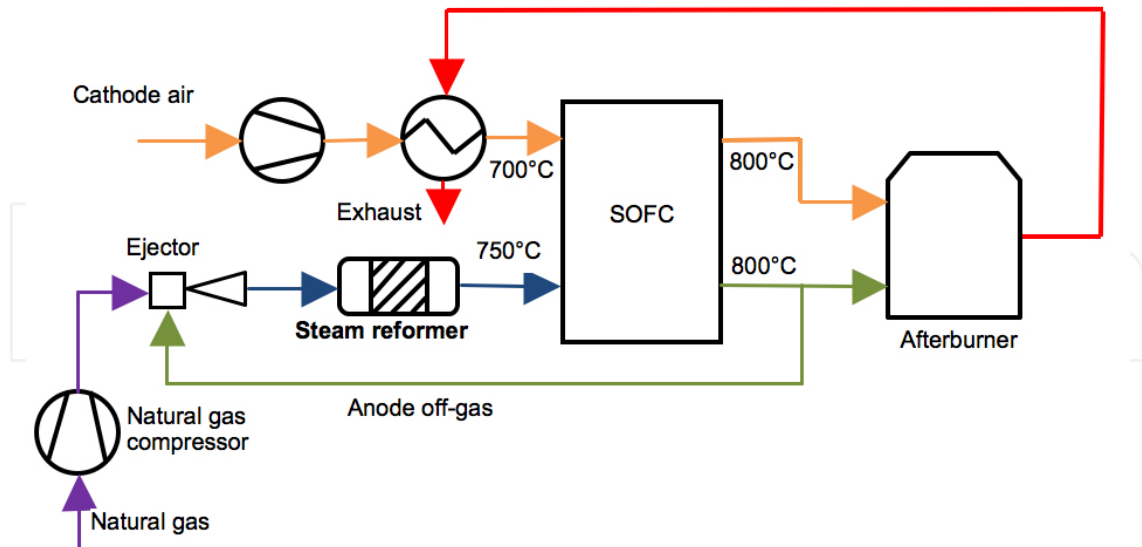


Figure 4. System with recirculation based on an ejector

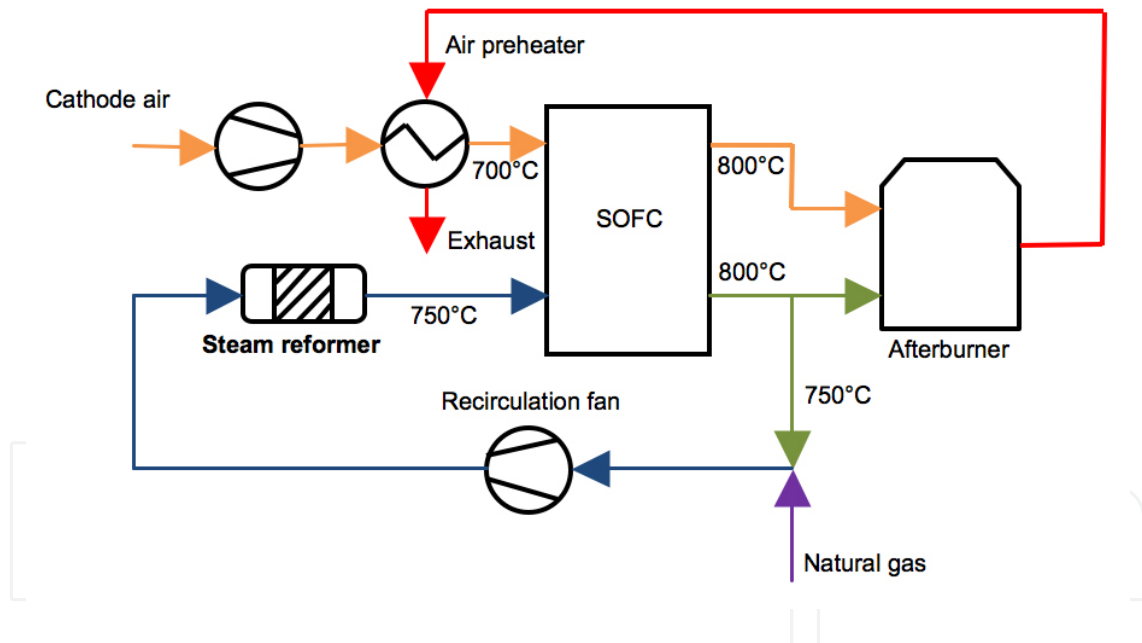


Figure 5. System with recirculation based on a high-temperature fan

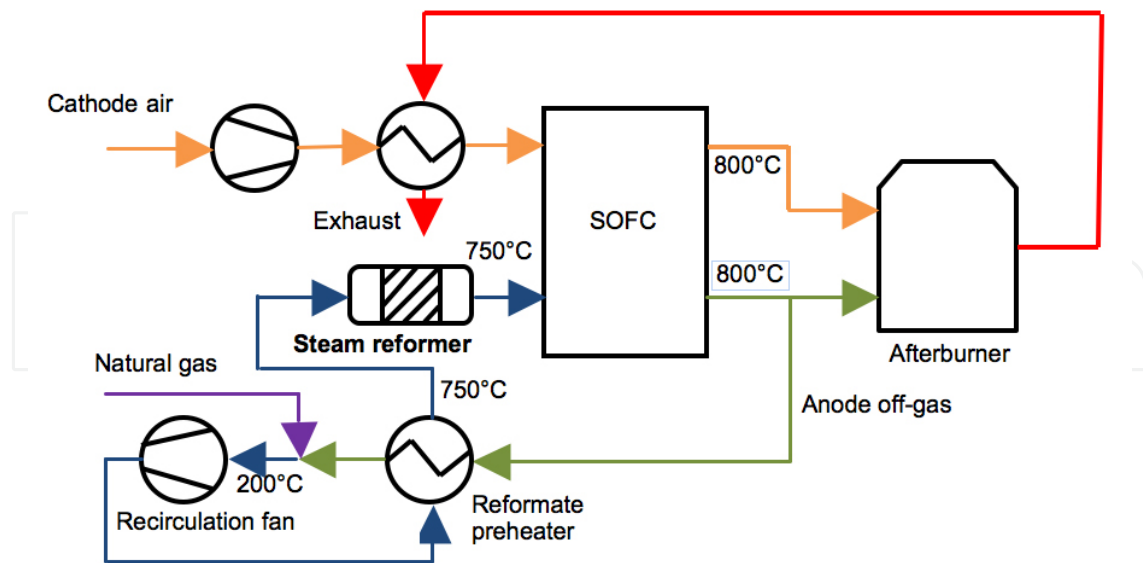


Figure 6. System with recirculation based on a low-temperature fan

3.2. 2- and 3D modeling and computational fluid dynamics codes

In 1-, 2- and 3D models, space-dependent governing equations are being solved. In case of three-dimensional approach, mathematical formulas are usually written in form of partial differential equations. Different methods can be used for solving the resulting set of equations. In 1D approach, ordinary differential equations may be encountered, and solution can be easily found with simple codes or even analytically. Complex 3D models of SOFC stack are useful for heat and mass exchange modeling [29]. With high fidelity models, different heat exchange means can be studied, and cell voltage under inhomogeneous temperature distribution can be found. Space-continuous models can be applied for material studies and evaluation of process losses. Time-dependent thermal processes can be studied in similar way to proposed nearly twenty years ago by Achenbach [30]. In his work, numerical tool was used to investigate heat conductivity of stack made of ceramic and metallic plates. With the proposed methodology it was possible to find the overall heat conductivities of the combined SOFC assembly. Additionally, the model was applied to evaluate influence of thermal radiation and the total heat losses from the stack. Such studies are crucial for evaluation of overall system performance, and can indicate dangerous operational modes, which should be avoided. Several analytical models of pressure and flow distribution in the stack have been presented [59,60]. The results have been compared to 3D CFD model, showing accuracy sufficient for engineering calculations. However, analytical models are typically applicable only to no-load, isothermal stack conditions.

Significant computational power is required to implement fully-3D CFD combined models of the SOFC stack and auxiliary system components. Computational time requirements limits complex optimization of such cases. In particular, when optimization of 3D models of system sections is necessary to approximate integration of SOFC stack with pre-heaters or reform-

ers, engineering accuracy approximations are often implemented. 3D non-CFD numerical model of SOFC stack has been applied to improve the thermal management of SOFC system through radiant heat transfer from the stack walls to adjacent air preheater panels [61].

In this study, options for minimizing axial and in-plane temperature gradients in the stack have also been identified. The results of subsequent tests, verifying modeling results, suggested that the use of radiation-based approach significantly improves the management of stack-generated heat [62].

Since porous body, representing electrochemically active part of the SOFC stack, is impermeable in directions other than flow direction in gas channels, simplifications of the 3D CFD stack model is possible, including 2D CFD model with the porous body approach (see Fig. 7). Periodical and ordered geometry of reactant channels in the stack, allows treatment of stack geometry as a porous body, with porosity defined as a ratio of channels cross-sectional area to stack cross-sectional area [63]. In the study, 2-D and 3D CFD SOFC stack models with internal manifolds have been implemented to simulate flow distribution under electric load conditions for the selected fuels. The semi-empirical model of electrochemical kinetics has been implemented. Typical flow arrangements of the inlet and outlet gas supply manifolds (U-flow, Z-flow) have been evaluated, including effects associated water-shift reaction and finite-rate of internal reforming of methane in the stack.

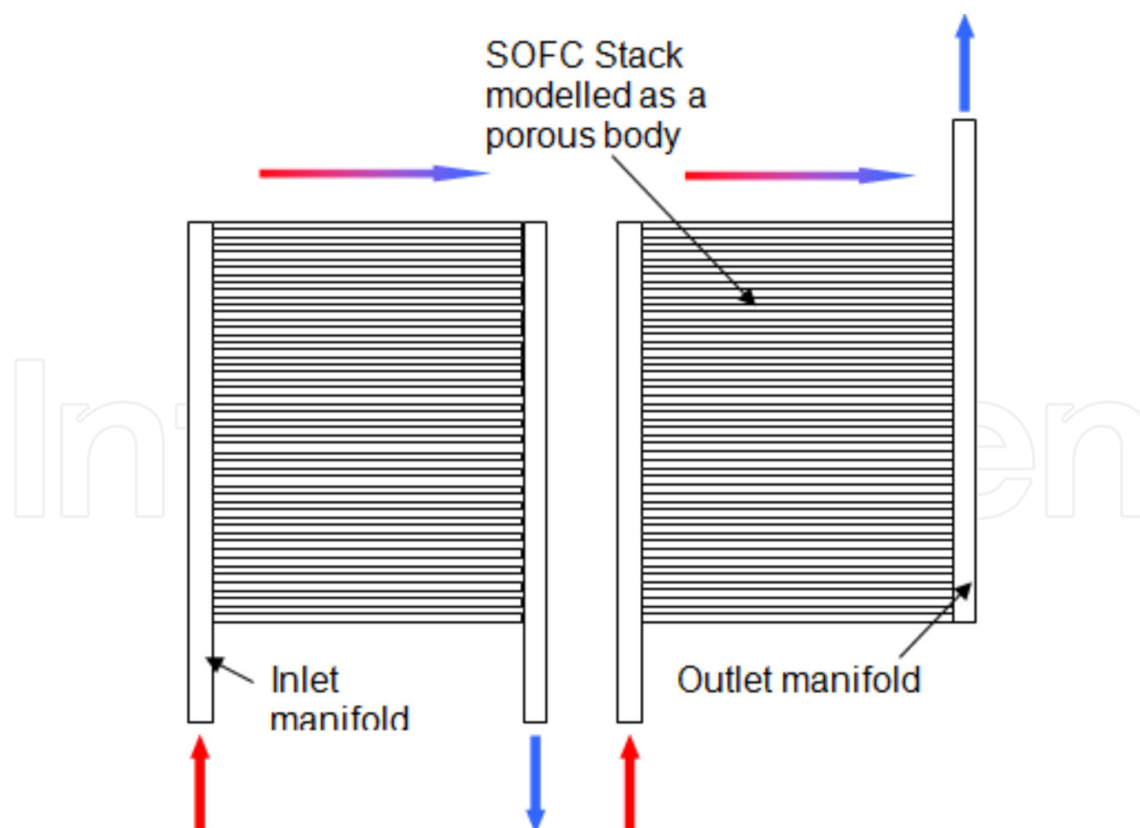


Figure 7. Stack representation in the 2D/3D CFD porous body approach

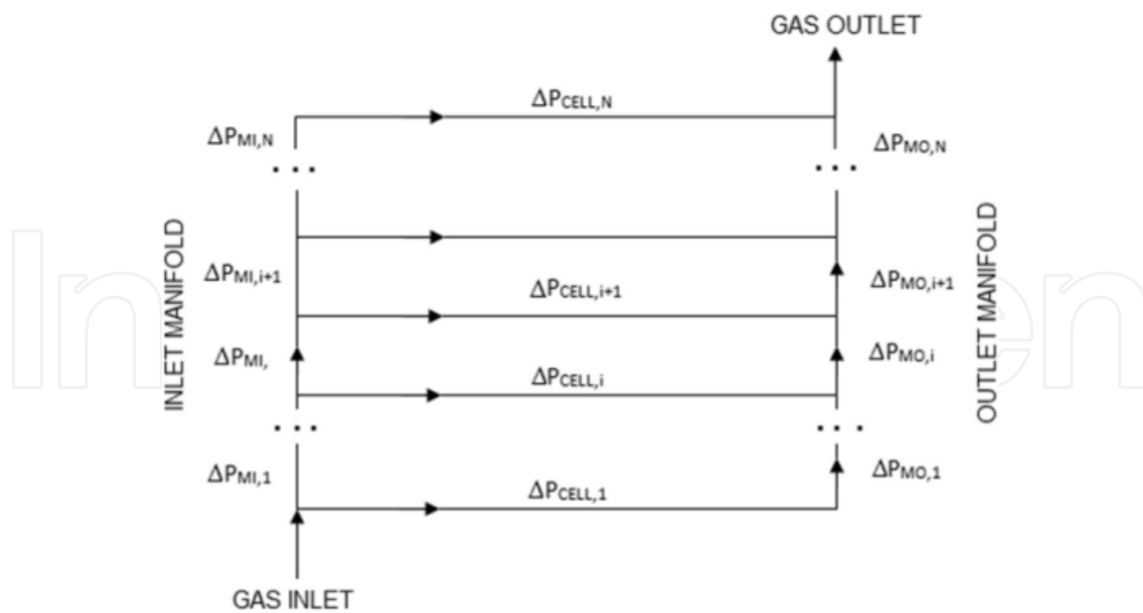


Figure 8. Stack representation in the hydraulic network approach

In yet another approach to SOFC stack modeling, so-called hydraulic network approach [64], pressure drop is calculated separately for each manifold section and reactant channel section, as shown in Fig. 8. The pressure drop is calculated based on the Darcy's friction factor, incorporating local geometry and stream characteristics. The hydraulic model approach has been implemented for the planar, rectangular geometry of the fuel cells. In the model, pressure drop is calculated separately for each manifold section and cell section:

$$\Delta P_i = f_D \frac{L_i \rho_i V_i^2}{D_i} \quad (4.1)$$

where:

f_D Darcy's friction factor

$f_D = K/Re$ for the laminar flow and $f_D = \varepsilon/D$ for the turbulent flow

ΔP_i pressure drop in the manifold section or cell section [Pa]

L length of the manifold section or cell section [m]

ρ_i gas density [kg cm^{-3}]

V_i gas velocity [m s^{-1}]

D hydraulic diameter [m]

K constant (64 for the circular channels)

ε/D relative roughness of the channel

Re Reynolds number

Additional pressure losses are calculated for the flow obstacles, such as dividing/combining flows at the manifold/reactant channel junctions, as:

$$\Delta P_i = K_{tot} \frac{\rho_i V_i^2}{2} \quad (4.2)$$

The resulting system of nonlinear equations is solved numerically for each of the flow loops:

$$\Delta P_{MI,i} + \Delta P_{CELL,i+1} - \Delta P_{CELL,i} + Q \cdot \Delta P_{MO,i} = 0 \text{ for } i=1 \dots N-1 \quad (4.3)$$

Numerical results show good convergence with analytical models (Fig. 9). The hydraulic networks approach is also applicable to SOFC stack modeling under electric load conditions.

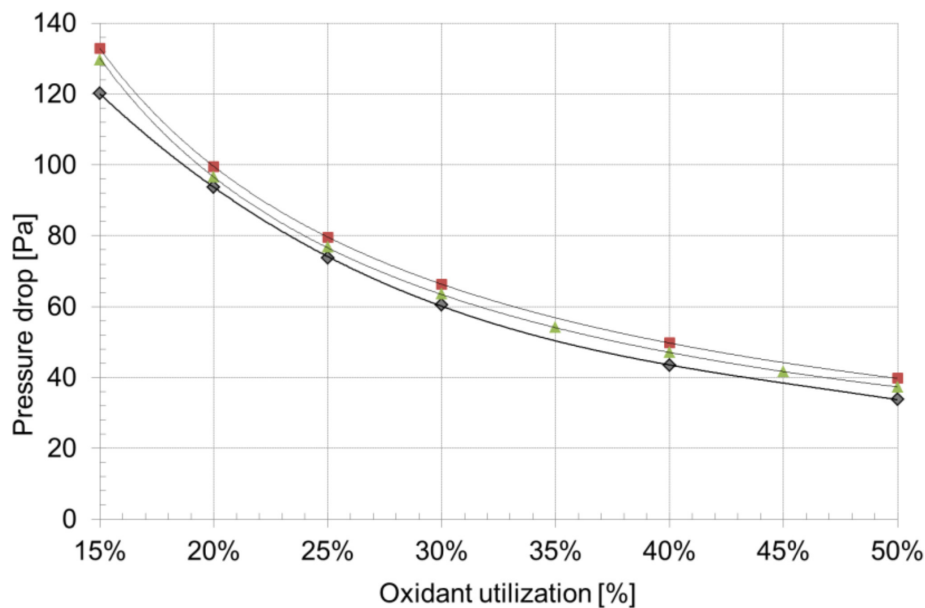


Figure 9. Comparison of pressure drop across the cathode side of the SOFC cell for a range of flows corresponding to a range of oxidant utilizations (▲ – hydraulic model results; ◆ – measurements, 295 K; ■ – 3D CFD simulation results)

Computational fluid dynamic system can be also used for system integration [2]. The coupling different models in one simulator can provide insight into operation of system components such as BoP devices, fuel processor, tail gas combustor, and SOFC stack. Time scale selection for the modeling should be done with caution. As has been noted by Tanaka et al. [29], certain fluctuations during small-scale co-generative SOFC-based unit operation occur. Authors performed detailed uncertainty estimation for 10 kW class units fed with town gas. Research was focused on evaluation of possible fluctuations, including changes in fuel quality over time (i.e. deviation of HHV from the nominal value), flow variations, precision of measurement equipment and other factors. The results indicate that the electrical efficiency of system can be determined with 1.0% relative uncertainty at 95% level of confidence for

such system. However, it should be noted that fuel cells are generally believed to operate quite stable when compared to other energy conversion techniques [31].

3.3. Fuel processing technologies

It is well known that the main advantage of solid oxide fuel cells is the ability to operate with number of different fuels including alcohols [32], hydrocarbons [31], pure hydrogen [33,21,31], biofuels [34] and energy carriers which can be converted to hydrogen-rich gas, including ammonia [35] and dimethyl ether [36]. Nonetheless, in order to assure high performance operation of a fuel cell stack, by limiting cells degradation, proper fuel processing has to be selected. As recently reported by Leone et al. [40] different fuel processing technologies may be used for fuel cell-based system, however reforming technique can influence cell operating conditions and selection should be made taking into account different factors.

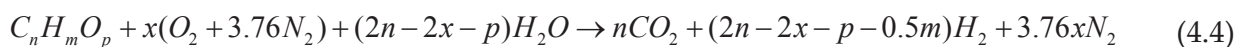
Generally, three different technologies can be distinguished for converting fuel before it enters the SOFC stack: catalytic partial oxidation (CPOX), steam reforming (SR) and autothermal reforming (AT). In certain cases these processes can be accompanied by fuel clean-up stage as it is usually done for fuels with significant H₂S content.

The important part of SOFC system operation is direct thermal integration of stack and fuel reforming. Different implementations have been proposed and corresponding modeling studies performed:

1. Intermediate indirect reforming plates (IIR) can be directly integrated with the SOFC stack [45,46]. In this approach, fuel reforming plates are integrated with the stack structure and separated with one or more fuel cells. Reformed fuel from the reforming plates is redirected to fuel inlet of the adjacent cell(s).
2. Direct internal reforming (DIR) is often implemented, taking advantage of catalytic properties of the SOFC anode material [47]. In this approach fuel is directly reformed on the anode side of the fuel cell. Pre-reforming of the fuel might be necessary in some cases to avoid overcooling of the fuel inlet stack region, particularly for the fuel with high methane content.
3. Thermal integration of SOFC stack and fuel reformer can also be implemented with thermal radiation/convection/conduction conjugate heat transfer between SOFC stack(s) and reformer. In this approach, fuel reformer is placed in a direct vicinity of the stack(s).

In this subsection, theory of different fuel processing technologies will be briefly discussed.

Partial oxidation reaction proceeds with the presence of catalyst can be written in a general form for any hydrocarbon [37]



where x is the oxygen to fuel molar ratio. This ratio defines the required amount of water for carbon to carbon monoxide conversion, amount of generated hydrogen, and molar concen-

tration of hydrogen in the reaction products. For $x = 0$ the reaction becomes an endothermic steam reforming, and for $x = 12.5$ it corresponds to a combustion process. Partial oxidation reaction should be controlled in such way, that overall thermal balance would be exothermic. Simple calculations lead to conclusion, that for a low value of x coefficient, higher amounts (or concentrations) of hydrogen should be expected. The main reason for using catalyst is the reduction of the process temperature. Reaction described by equation (1) to proceed without catalyst, however temperature of about 1000°C is required in such case. Because of that fact in most commercial applications, including SOFC-based systems, catalyst is used.

Second method for turning different fuels into hydrogen-rich gas is the steam reforming. In most fuel cell applications, reaction proceeds at high temperature with addition of water vapor. Typical products of steam reforming include hydrogen and carbon dioxide. Ideal reaction can be written for any hydrocarbon fuel fed in the following form:



In most technological processes, steam reforming comprises two stages which can be written for the simplest hydrocarbon in a form:



and



Where equation (4.6) is strongly endothermic and (4.7) is slightly exothermic, therefore the overall reaction requires heat delivery. Typically, steam reforming of gases can also be done as a catalyst-supported process. Usually a metallic nickel catalyst [38,39] either Ni/Al₂O₃ or Ni on refractory material, containing 5-30% of Ni are used. Lifetime of a catalyst strongly depends on quality of gases converted in the steam reformer, so-called poisoning is usually the main process leading to rapid performance deterioration. In order to ensure long lasting operation of the catalyst, poisonous impurities should be removed prior the reforming process.

Next to CPOX and SR, internal reforming is also mentioned as an interesting processing technology and the most economical way to convert hydrocarbon fuels for tubular and planar SOFCs. Despite the fact that process has number of advantages, it may lead to high temperature variations in the fuel cell and stack [41]. Highly endothermic character of the reaction is responsible for local cooling of the cell material leading to cracking and rupture. In a similar way, CPOX reaction along the cell is often claimed to be responsible for cell overheating which can compromise the ceramic material stability in a similar way as internal reforming. Even though, internal reforming is allowed to a certain extent, it is believed that thermal decomposition of higher hydrocarbons may lead to carbon formation on the anode compartments [30]. Usually, limitation on the fraction of higher hydrocarbons is imposed by

material issues (endothermic reforming reaction) and possibility of carbon deposition to occur. Recent study presented in 0D modeling section and available literature [42,43] clearly indicates that steam reforming is the most efficient technology for bioethanol, methane and other hydrocarbons conversion into hydrogen rich-gas. Arteaga et al. [44] performed thorough evaluation of different fuel processing technologies particularly for SOFC application also finding steam reforming the most suitable. Comparison of different fuel processing technologies for biogas and methane was previously done and reported [53]. It was clearly indicated that steam reforming is the optimal selection for micro-CHP units with SOFCs.

As it was discussed in previous section, systems with SOFCs require fuel processing. In most cases steam reforming would be selected, and in such system catalysts would be employed.

4. Control strategy for micro-CHP unit

Since micro-CHP unit of discussed type generated both electricity and heat, two control strategies are possible. Device can operate following electricity or heat/hot water demand. Generally it is believed, that the most optimal strategy is to control electricity generation, considering heat as a by-product which can possibly be stored in sufficiently large water tank. In available literature, different tank sizes were considered. In design of micro-CHP system with power output of about 2 kW by Kupecki and Badyda [5], tank with volume of 600 liters was considered. At average storage temperature of 55° C, the total of about 28 kW_{th} can be stored in the tank. This volume was selected based on availability of off-the-shelf products, its reasonable price and sufficient heat capacity. Surprisingly, some authors [65] suggest selection of much larger size like 1000 or even 3000 liters. From the product development point of view, customer expectations and required compact size, this is an a way too large volume. Moreover, according to authors' own calculations, selection of such a big vessel has negligible economical gain, and in all cases can lead to increase of capital cost of the system. Price of hot water storage tanks increases exponentially with the capacity increase, therefore considerations of volumes above 600 liters should not have place. Additional aspect of control strategy selection depend on current conditions, including generation price and cost or resources.

In a recent study [66] control strategy for the highest energy savings for 20 households using 0.7 kW micro-CHP systems with SOFC was evaluated. Mixed-integer linear programming was used to optimized control for a case, and when each of households has a different consumption. They clearly found, that electrical load-following is the best strategy, allowing the highest energy-saving effect. Authors also pointed out that wastage of surplus hot water is possible in the summer season, but this can be avoided by selection of slightly larger water tank.

5. Modeling the dynamic behavior of a singular Solid Oxide Fuel Cell

5.1 Dynamic oriented model of SOFC

The mathematical model of SOFC for steady state calculations was presented in a few previous papers [73,74,75,76,77,78,79,80]. In this section only dynamic oriented relationships are included and commented on.

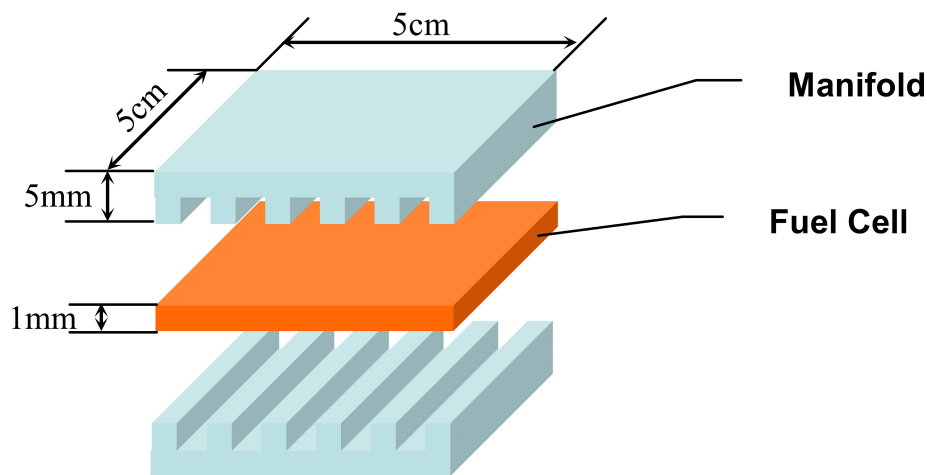


Figure 10. Dimensions of fuel cell plate and the manifolds

As an object for modeling, a singular fuel cell is chosen with dimensions of $5 \text{ cm} \times 5 \text{ cm}$ and thickness of 1 mm (see Fig. 10). It was assumed that the manifolds (for fuel and oxidant) are identical.

Some processes which occur during fuel cell operation are very rapid, thus they can be assumed to be time independent compared to others. The following processes are assumed to be time independent:

1. Electrical processes
2. Electrochemical processes
3. Pressure changes

For those processes only the static equations were utilized.

Fig. 11 presents a concept of a model of Solid Oxide Fuel Cell, the fuel cell is equipped with two inlet streams and two outlet streams. Processes which occur during fuel cell operation can be divided into three steps: capture of oxygen atoms from the delivered oxidant (air), oxygen ions passing through the electrolyte layer, and the ions escaping and reacting with the delivered fuel. Material aspects play a crucial role here [68].

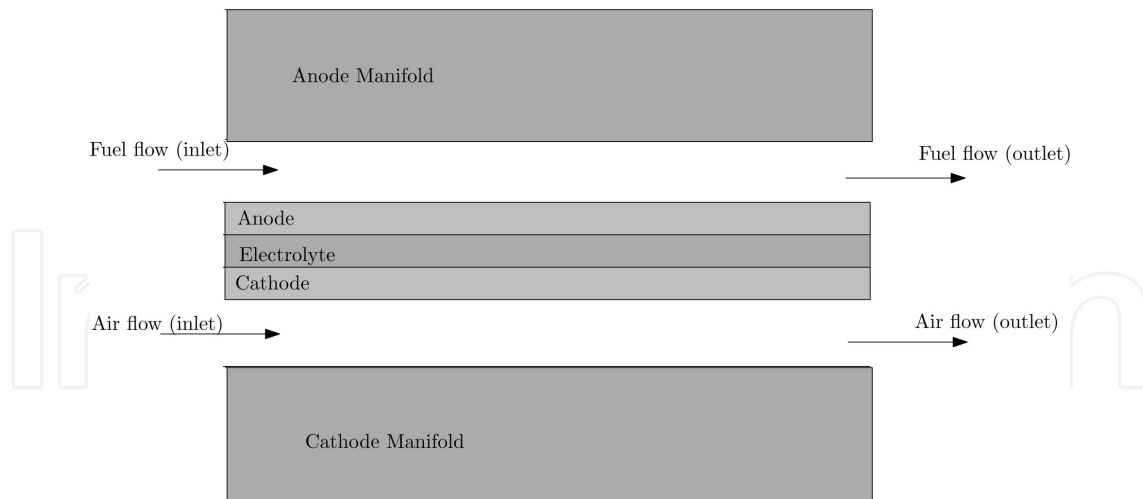


Figure 11. A concept of a model of Solid Oxide Fuel Cell

The fuel cell presented in Fig. 11 can be reduced to an 0D model. This is the simplest approach, but generates a model of the same class as models of other equipment (compressors, pumps, heat exchangers). The set of equations for the 0D model is as follows:

$$\left\{ \begin{array}{l} \frac{dT_{Cell}}{dt} = \frac{\dot{Q}_{Oxidant} + \dot{Q}_{Fuel} - 2 \cdot \dot{Q}_{Surrounding} - P_{SOFC} + \dot{Q}_{Fuel}}{2 \cdot C_{Manifold} + C_{Fuel} + C_{Oxidant} + C_{Cell}} \\ \frac{dp_{Cathode,Out}}{dt} = \frac{\dot{m}_{Cathode,In} - \dot{m}_{Cathode,Out}}{V_{Cathode}} \\ \frac{dp_{Anode,Out}}{dt} = \frac{\dot{m}_{Anode,In} - \dot{m}_{Anode,Out}}{V_{Anode}} \end{array} \right. \quad (6.1)$$

where:

$$\dot{Q}_{Oxidant} = \dot{m}_{Oxidant} \cdot c_{p,Oxidant} (T_{Cathode,In} - T_{Cell}) \quad (6.2)$$

$$\dot{Q}_{Fuel} = \dot{m}_{Fuel} \cdot c_{p,Fuel} (T_{Anode,In} - T_{Cell}) \quad (6.3)$$

$$\dot{Q}_{Surrounding} = k_{Surrounding} \cdot A_{Cell} (T_{Cell} - T_{Surrounding}) \quad (6.4)$$

$$P_{SOFC} = E_{SOFC} \cdot I_{SOFC} \quad (6.5)$$

$$\dot{Q}_{Fuel} = \dot{m}_{Fuel} \cdot HHV_{Fuel} \cdot \eta_f \quad (6.6)$$

$$C_{Manifold} = m_{Manifold} \cdot c_{p,Manifold} \quad (6.7)$$

$$C_{Cell} = m_{Cell} \cdot c_{p,Cell} \quad (6.8)$$

Factor	Value	Comment
Specific heat of oxidant, $c_{p,Oxidant}$ [kJ kg ⁻¹ K ⁻¹]	1.156	Electrochemistry air
Specific heat of fuel, $c_{p,Fuel}$ [kJ kg ⁻¹ K ⁻¹]	15.25	hydrogen
Heat transfer coefficient to surrounding, $k_{Surrounding}$ [W m ⁻² K ⁻¹]	0.1	fuel cell is isolated
Higher Heating Value of fuel, HHV_{Fuel} [MJ kg ⁻¹]	144	hydrogen Thermal balancing
Specific heat of interconnector material, $c_{p,Manifold}$ [kJ kg ⁻¹ K ⁻¹]	0.5	LaCrO ₃
Specific heat of fuel cell, $c_{p,Cell}$ [kJ kg ⁻¹ K ⁻¹]	0.5	YSZ
Interconnector weight in relation to fuel cell area [kg m ⁻²]	20.3	
Fuel cell weight in relation to fuel cell area [kg m ⁻²]	6	

Table 4. Selected factors of a dynamic oriented mathematical model of SOFC.

The factors used in the above equations are presented in Table 4.

Typical interconnects have a thickness of 3 mm [82], which gives 7.5 cm³ of material for fuel cell dimensions of 5 cm × 5 cm × 3 mm. Assuming that the interconnect is made from LaCrO₃, the interconnect weight is 50 g per fuel cell. The additional weight relates to the manifolds which deliver the working fluids—depending on the current architecture solution of the stack. In this study, it was assumed that the interconnect weight in relation to fuel cell area is 2.03 g cm⁻².

The typical channel within which working fluids are delivered has dimensions of 0.5 mm × 1.5 mm, and its length depends on the total fuel cell dimensions (5–8 cm). Usually, the distance between the channels are the same as the channels themselves. Assuming a planar fuel cell of dimensions of 5 cm × 5 cm, the channel volume is 0.5 mm × 5 cm × 5 cm = (17 × 17 × 1.5 mm × 1.5 mm × 0.5 mm) = 0.925 cm³ per each fuel cell side and in total 1.85 cm³ for the fuel cell. Relating the volume to the fuel cell area gives a value of 0.074 cm³/cm² of the channel volume in relation to fuel cell area.

Parameter	LaCrO ₃
Heat conductivity [67] [W m ⁻¹ K ⁻¹]	1.7–2.5

Coefficient of thermal expansion [72], $\Delta L/L/K$	$(2-8) \cdot 10^{-6}$
Density [71] [$g\ cm^{-2}$]	3–6.77

Table 5. Main material parameters of interconnector.

Working fluids velocities inside the channels depend on the channel dimensions and quantity of flows delivered. To provide an adequate time for reaction as well as mixing of reagents, the velocities of working fluids should be relatively low. Based on the authors' own calculations, the nominal velocities of working fluids are below $5\ m\ s^{-1}$, being on average $1.6\ m\ s^{-1}$. Due to such low velocities, the pressure drops along the channels can be omitted [69].

Parameter	Value
Specific fuel cell weight [$g\ cm^{-2}$]	0.6
Specific interconnect weight [$g\ cm^{-2}$]	2.03
Specific volume [$cm^3\ cm^{-2}$]	0.074

Table 6. Main material factors of the fuel cell related to fuel cell area.

5.2. Dynamic behavior of SOFC

5.2.1. The control strategy

During fuel cell operation there is a series of processes that affect its performance. The operator affects only some of them; the parameters subject to direct regulation are:

1. Temperature of inlet air
2. Temperature of inlet fuel
3. Quantity of inlet air
4. Quantity of inlet fuel
5. Electric current draw from the cell

The amounts of air and fuel supplied to the fuel cell should enable its proper operation, especially the behavior of the quantities of both fuel utilization and oxidant utilization. In addition, changes in certain parameters interact in a similar way: maintaining the desired temperature of fuel cells can be achieved by either reducing or increasing the amount of air and its temperature. Both of these parameters are related to each other (you cannot cool the cell with overly hot air, regardless of the amount). Selection of the optimal control strategy in this case is a key issue.

In this study, it was assumed that the fuel utilization factor is kept constant at the point of maximum efficiency (in fact at the laboratory scale it means only 4.5% for a fuel utilization factor of 12%). This means that inlet fuel mass flow is correlated with fuel cell current.

The most important parameter is cell temperature, which must be kept constant. The temperature is controlled by an inlet air mass-flow, which is regulated by a valve equipped with a PID regulator.

	K_p	K_i	K_d
PI	$\frac{1}{K \cdot T_0}$	$4.3 \cdot T_0$	
PID	$\frac{1 \cdot 36}{K \cdot T_0}$	$1.6 \cdot T_0$	$0.5 \cdot T_0$

Table 7. Optimal parameters of PID controller [70].

The singular PID controller is chosen to keep the fuel cell temperature at set point (800°C). The PID controls inlet air mass flow. Optimal PID parameters are listed in Table 7. For these parameters the optimal parameter settings for the PID controller of the fuel cell are determined:

- $K_p = 3.264$
- $K_i = 1.6$
- $K_D = 0.5$.

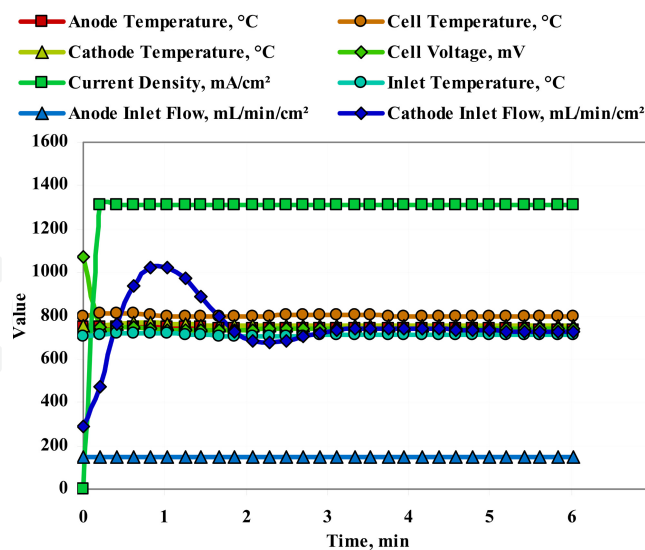


Figure 12. System response to a step change in charging current density (0–1.3 A/cm²) using PID

Fig. 12 shows the cell parameters change with a stepped increase in current density using the PID controller. It can be seen that the quality of control is very good (almost no distortion: 15°C), and the system reaches a steady state after about 4 minutes. The amount of air

fed to the cathode reaches $1000 \text{ ml min}^{-1}\text{cm}^{-2}$. Cell voltage drops to the value of 0.75 V and remains without significant change.

5.2.2. Start-up

An external source of heat is required to support the start-up of a fuel cell. The simplest solution is to use the burner boot to warm the cell to a temperature which enables it to work independently. During fuel cell start-up acceptable temperature differences should be preserved, with the assumed values being:

- 45°C between inlet and outlet temperatures of working fluids
- 90°C between working fluid temperature and fuel cell temperature

An active start-up system is proposed, comprising regulating the temperature of gases supplied to the cells depending on cell temperature.

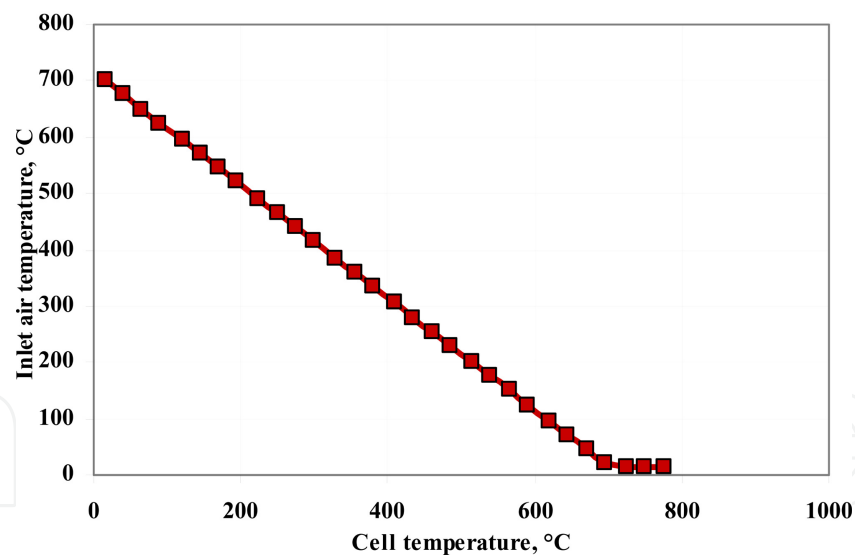


Figure 13. Correlation of air temperature used for heating the cell with cell temperature was applied during the simulation starting from cold state

The amount of air used to heat the cells was determined as the nominal point. The temperature of the air is correlated with the cell temperature according to the relation with which the air temperature decreases from the value of 700°C in proportion to the increase in cell temperature (see Fig. 13).

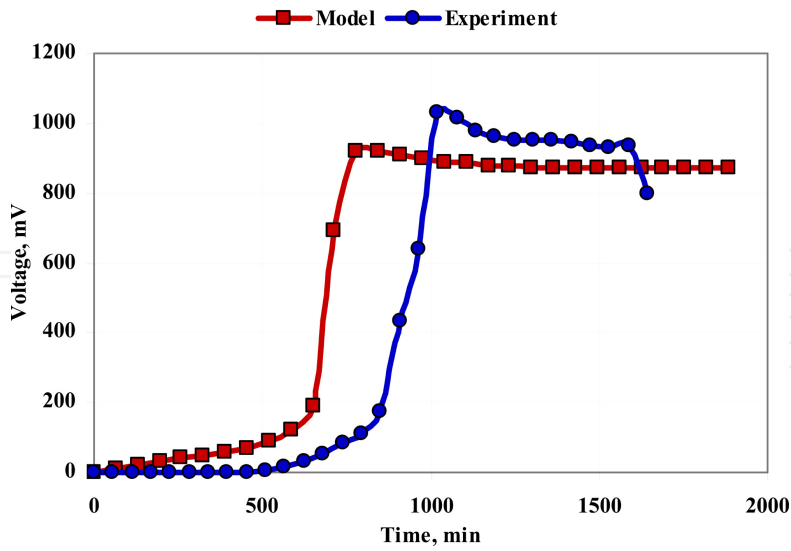


Figure 14. Comparison of the simulated start-up procedure with the results obtained from experiments [80]

Fig. 14 presents a comparison of the simulated cell voltage during start-up against the real values (data [80]). The two cells differ in structure as well as in the procedures used during start-up but, qualitatively speaking, the modeled start-up is a very close approximation to the reality.

5.2.3. Continuous operation and changes in power

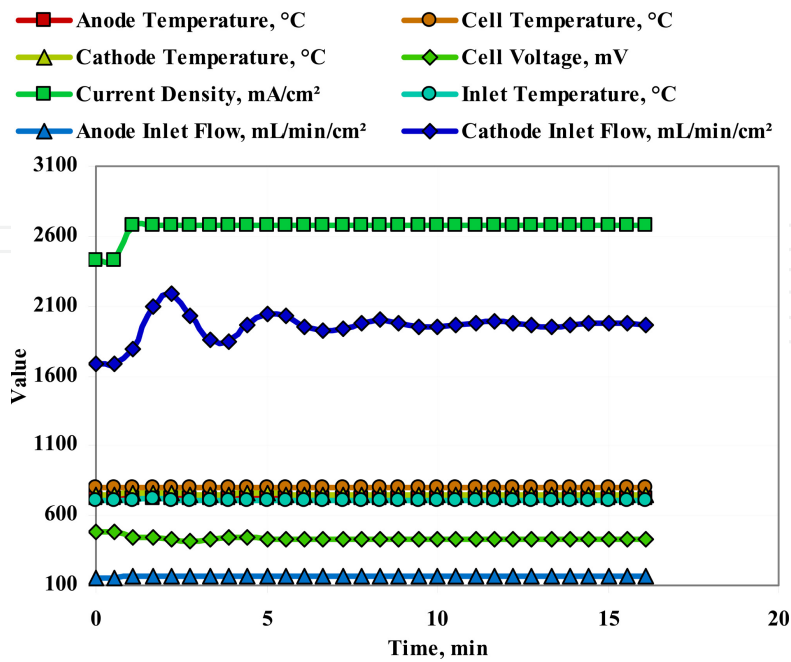


Figure 15. Changes of the fuel cell operating parameters during load increases by 10%

The results of simulated rapid increase in power by 10% are shown in Fig. 15. The control system keeps all key parameters in acceptable ranges. Larger changes are noted only for current density (which increases from 2.43–2.68 A cm⁻²), and the air flow rate, which is the result of regulation and oscillates between 1600–2200 ml min⁻¹cm⁻² finally stays at 2000 ml min⁻¹cm⁻².

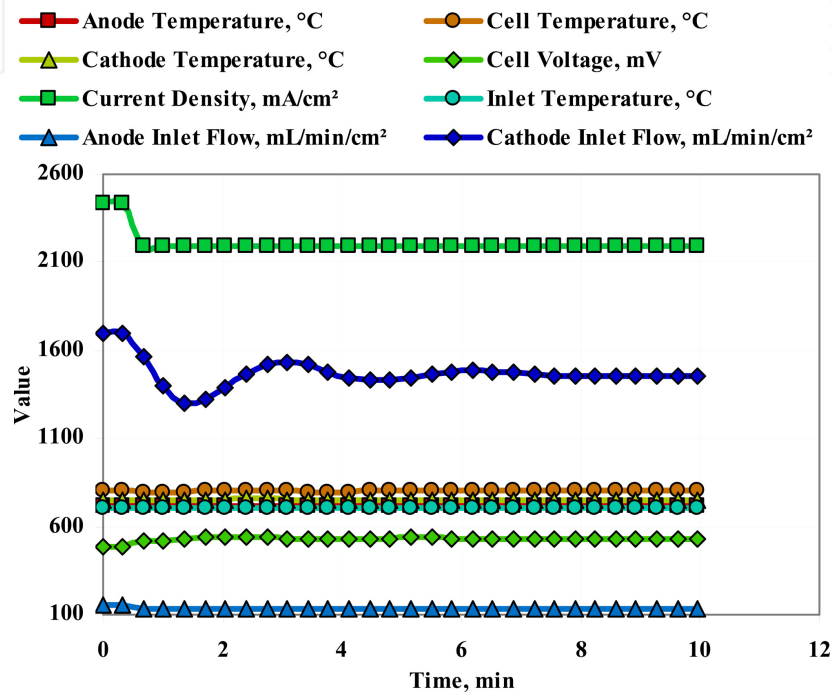


Figure 16. Changes of the fuel cell operating parameters during load decreases by 10%

The results of simulated rapid decrease in power by 10% are shown in Fig. 16. The control system keeps all crucial parameters in the acceptable ranges, so that most of the parameters practically do not change themselves. Larger changes are noted only for the current density (which increases from 2.43–2.19 A cm⁻²), and the air flow rate which is the result of regulation and oscillates between 1300–1700 ml min⁻¹cm⁻² finally stays at 1400 ml min⁻¹cm⁻².

5.2.4. Loss of load

The most likely emergency scenario is a sudden loss of load resulting from load shut down (e.g. activation of the safety switch). In this case the fuel cell should be left to idle.

Fig. 17 presents the simulated behavior of a fuel cell reacting to a sudden loss of load. The fuel cell parameters stabilize after about 4 minutes and the cell goes into idle mode. The cell temperature reaches 807°C, which seems to be a safe value.

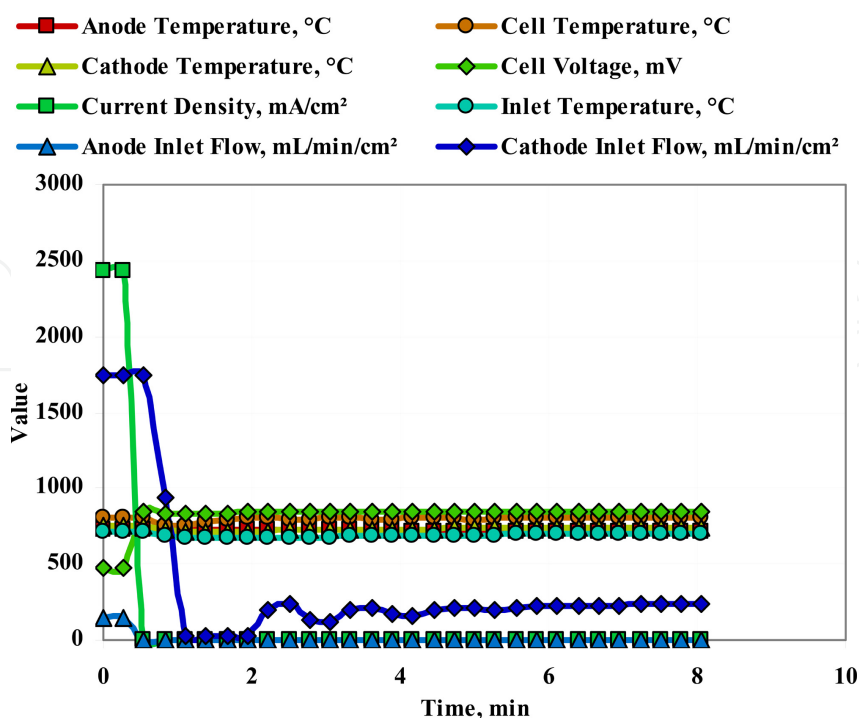


Figure 17. Simulated behavior of a fuel cell reacting to a sudden loss of load

On the basis of the simulation it can be concluded that the fuel cell is relatively resistant to a sudden loss of load in the presence of a proper control system.

5.2.5. Shut down

During normal operation the fuel cell is able to resist a sudden loss of load. Therefore no special procedures are required to shut down the fuel cell unit. Additional procedures should be used to cool down the fuel cell to ambient temperature. The best option seems to be using a PID controller with variable temperature settings.

Fig. 18 shows the fuel cell characteristics with stepped increase in the quantity of air supplied to the cathode to its maximum value (6000 ml min⁻¹cm⁻²). The cathode part of the fuel cell loses heat relatively quickly, reaching ambient temperature after about 10 minutes. By contrast, at the anode side, there is no fuel flow and cooling takes far longer (after 30 minutes the temperature drops by only a few degrees). In total, this leads to very large temperature differences between the anode and cathode side (almost 600°C).

In order to shut down the fuel cell, the flows on both the anode and cathode sides need to be maintained. The simplest solution is to maintain the fuel stream on the anode side, which otherwise experiences a loss of fuel. Another solution is to provide another gas, but it should be an inert gas (the use of air may result in oxidation of the anode surface).

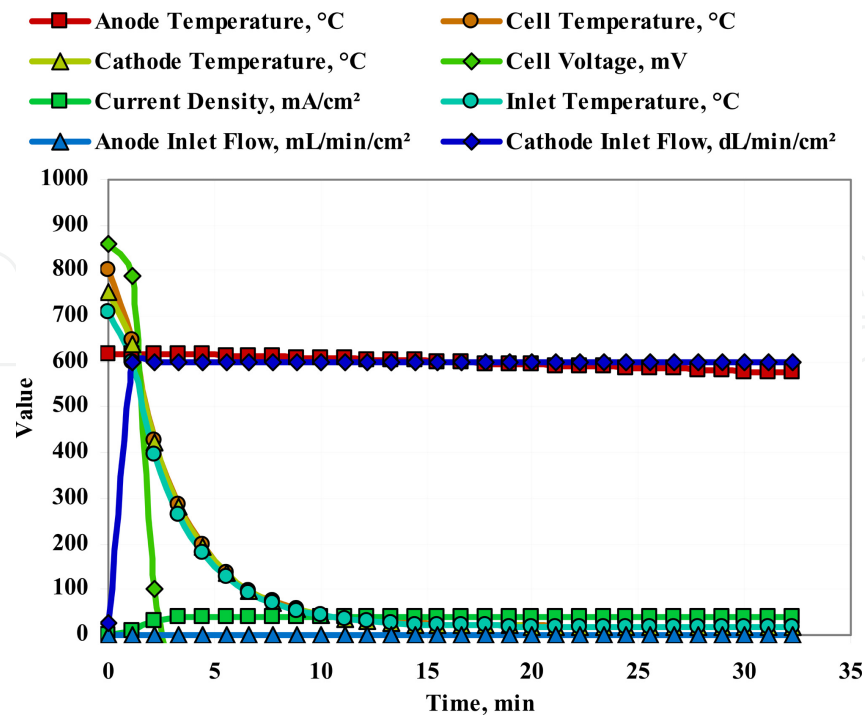


Figure 18. Fuel cell parameters during shut down procedure based on maximizing cathode flow (air side)

5.3. Discussion

The control strategy for a singular solid oxide fuel cell is proposed. The strategy is based on a singular PID controller which controls the amount of air delivered to the cathode side of the fuel cell. Additionally, fuel mass flow is correlated with current density to achieve a fixed fuel utilization factor. In fact, the efficiency of the singular laboratory scale fuel cell unit is relatively low, as is the fuel utilization factor.

The start-up procedure of the fuel cell must be supported by an external source of heat. Theoretically speaking, it is possible to heat up the cell until the point at which it starts to generate some voltage (practically, above 0.4 V) and then the fuel cell should be able to heat itself up to working temperature by the applied external load. The simulations performed do not confirm this theoretical speculation. After the load is applied, the voltage drops and no current can be drawn. Thus, adequate correlation of air inlet temperature with cell temperature is proposed in order to reach the nominal temperature. The simulated start-up was compared with the experimental data, with satisfactory results.

During normal operation, the proposed control system keeps all fuel cell parameters within acceptable ranges—there are no consequences following a rapid increase/decrease of load by 10%.

The one conceivable emergency scenario was analyzed: rapid loss of external load. The control system keeps the key parameters at acceptable levels (e.g. cell temperature reaches 807°C).

The simulated shut down procedure was unsuccessful: the PID controller was used to cool the fuel cell, but it only influenced air flow, causing an extremely high temperature gradient. Additional procedures must be applied to cool the fuel cell properly.

6. Conclusions

Different mathematical models are useful for evaluation and prediction of fuel cells and entire system performance. In all cases, specific application-related criteria are selected for development of numerical tool.

Development of advanced energy systems, including micro-CHP units, under various operating conditions is possible only with high-fidelity numerical simulator. Tool has to be validated against available experimental data. In certain cases, numerical modeling is not possible without supporting experimental measurement.

Different time- and length-scales can be covered with dedicated models, ranging from 0D up to complex full-3D tools. Steady state can be evaluated with available engineering software, including computational fluid dynamic tools.

Analysis of chemical and electrochemical reactions taking place during SOFC operation requires specific knowledge and in most cases detailed models are needed. Spatial configuration and influence of geometry can only be studied with space-continuous models or number of simplifications is required.

Based on mathematical modeling, an analysis of the dynamic operation of a singular fuel cell is presented. Based on the analysis a few cases relating to the cell were simulated:

- Start up
- Continuous operation (with power changes in the range of +/-10%)
- Shut down, and
- Emergency scenario (loss of load)

In almost all cases, the singular PID controller is able to keep the fuel cell operation within a safe range. Special procedures are required during start up and shut down. During start up, external heat sources are required to warm the cell to operational temperature. It is proposed that air temperature be correlated to cell temperature. As regards the shut down procedure, a change in fuel cell configuration is required—an inert gas instead of fuel must be delivered in order to cool the cell.

The start up procedure was compared against available experimental data with satisfactory results, qualitatively speaking.

Acknowledgements

Support from the European Regional Development Fund and Ministry of Science and Education under the project no. UDA-POIG.01.01.02-00- 016/08-00, from the National Centre for Research and Development under the project Advanced Technologies for Energy Generation, and European Social Fund through the “Didactic Development Program of the Faculty of Power and Aeronautical Engineering of the Warsaw University of Technology” are gratefully acknowledged.

Author details

Jakub Kupecki^{1,2*}, Janusz Jewulski¹ and Jarosław Milewski²

*Address all correspondence to: jakub.kupecki@ien.com.pl

1 Fuel Cell Department, Institute of Power Engineering, Poland

2 Institute of Heat Engineering, Warsaw University of Technology, Poland

References

- [1] European Commission . (2004). 2004/8/EC Directive on the promotion of cogeneration based on a useful heat demand in the internal energy market and amending directive 92/62/EEC.
- [2] Kattke, K. J., Braun, R. J., Colclasure, A. M., & Goldin, G. (2011). High-fidelity stack and system modeling for tubular solid oxide fuel cell system design and thermal management. *Journal of Power Sources*, 196, 3790-3802.
- [3] Blum, L., Deja, R., Peters, R., & Stolten, D. (2001). Comparison of efficiencies of low, mean and high temperature fuel cell systems. *International Journal of Hydrogen Energy*, 36, 11056-11067.
- [4] Mekhilef, S., Saidur, R., & Safari, A. (2012). Comparative study of different fuel cell technologies. *Renewable and Sustainable Energy Reviews*, 16, 981-989.
- [5] Kupecki, J., & Badyda, K. (2011). SOFC-based micro-CHP system as an example of efficient power generation unit. *Archives of Thermodynamics*, 32(3), 33-42.
- [6] DOE Energy Efficiency and Renewable Energy Information Center. (2008). Comparison of fuel cell technologies.
- [7] Mai, A., Sfeir, J., & Schuler, A. (2007). Status of sofc stack and systems development at Hexis. Fuel Cell Seminar 2007 proceedings 5-8.11. 12.

- [8] Schuler, A., Nerlich, V., Doerk, T., & Mai, A. (2010). Galileo 1000N—status of development and operation experiences. *Proceedings of 9th European Solid Oxide Fuel Cell Forum*, 2, 98.
- [9] Foger, K. (2010). Commercialisation of CFCL's residential power station Blugen. *Proceedings of European Fuel Cell Forum, Lucerne*, 2, 22-29.
- [10] Brennstoffzellenheizgerate fur die Hausenergieversorgung: Die Zukunft der Kraft-Warme- Kopplung. (2008). (2036197-204), VDI-Bericht.
- [11] Klose, P. (2009). Pre-series fuel-cell-based m-CHP units in their field test phase. In 11th Grove Fuel Cell Symposium. London.
- [12] Pawlik, J., & Klaschinsky, H. (2008). Das Viessmann Brennstoffzellen- Heizgerat. (2036189-196), VDI-Bericht.
- [13] Toshiyuki Unno JX Nippon. personal communication.
- [14] Kirubakaran, A., Jain, S., & Nema, R. K. (2009). A review of fuel cell technologies and power electronic interface. *Renewable and Sustainable Energy Reviews*, 13, 2430-2440.
- [15] Dunbar, W. R., Lior, N., & Gaggioli, R. A. (1991). Combining Fuel Cells with Fuel-Fired Power Plants for Improved Exergy Efficiency. *Energy*, 16(4), 1259-1274.
- [16] Bedringas, K. W. (1997). Exergy Analysis of Solid-Oxide Fuel Cell (SOFC) Systems. *Energy*, 22(4), 403-412.
- [17] Chan, S. H., Ho, H. K., & Tian, Y. (2002). Modelling of simple hybrid solid oxide fuel cell and gas turbine power plant. *Journal of Power Sources*, 109, 111-120.
- [18] Harvey, S. P., & Richter, H. J. (1997). Gas turbine cycles with solid oxide fuel cells. Part I: improved gas turbine power plant efficiency by use of recycled exhaust gases and fuel cell technology. *Journal of Energy Resources Technology*, 116, 305-311.
- [19] Kupecki, J. (2010). Integrated Gasification SOFC Hybrid Power System Modeling: Novel numerical approach to modeling of advanced power systems. VDM Verlag Dr. Müller.
- [20] Grew, K. N., & Chiu, W. K. S. (2012). A review of modeling and simulation techniques across the length scales for the solid oxide fuel cell. *Journal of Power Sources*, 199, 1-13.
- [21] O'Hayre, R., Cha, S. W., Colella, W., & Prinz, F. (2005). Fuel cell fundamentals. Wiley.
- [22] Pasaogullari, U., & Wangm, C. (2003). Computational fluid dynamics modeling of solid oxide fuel cells. *Electrochemical Society Proceedings*, 07, 1403-1412.
- [23] Proceedings of hydrogen and fuel cells 2004, Toronto, Canada. Mathematical modeling of the transport phenomena and the chemical/electrochemical reactions in solid oxide fuel cells: A review. (2004).

- [24] Dagan, G. (1989). Flow and transport in porous formations. Springer.
- [25] Iwata, M., Hikosaka, T., Morita, M., Iwanari, T., Ito, K., & Onda, K. (2000). Performance analysis of planar-type unit SOFC considering current and temperature distributions. *Solid State Ionics*, 132, 297-308.
- [26] Bove, R., & Ubertini, S. (2006). Modeling solid oxide fuel cell operation: Approaches, techniques and results. *Journal of Power Sources*, 159, 543-559.
- [27] Lisbona, P., Corradetti, A., Bove, R., & Lunghi, P. (2007). Analysis of a solid oxide fuel cell system for combined heat and power applications under non-nominal conditions. *Electrochimica Acta*, 53, 1920-1930.
- [28] Karcz, M. (2009). From 0D to 1D modeling of tubular solid oxide fuel cell. *Energy Conversion and Management*, 50, 2307-2315.
- [29] Tanaka, T., Inui, Y., Urata, A., & Kanno, T. (2007). Three dimensional analysis of planar solid oxide fuel cell stack considering radiation. *Energy Conversion and Management*, 48, 1491-1498.
- [30] Achenbach, E. (1994). Three-dimensional and time-dependent simulation of a planar solid oxide fuel cell stack. *Journal of Power Sources*, 49, 333-348.
- [31] US Department of Energy, Office of Fossil Energy National Energy Technology Laboratory. Fuel Cell Handbook 7th Edition. (2004). EG G Technical Services, Inc.
- [32] Jiang, Y., & Virkar, A. V. (2001). A high performance, anode-supported solid oxide fuel cell operating on direct alcohol. *Journal of Electrochemical Society*, 148(7), A706-A709.
- [33] Yokokawa, H. (2003). Understanding materials compatibility. *Annual Review of Materials Research*, 33, 581-610.
- [34] Staniforth, J., & Ormerod, R. M. (2003). Running solid oxide fuel cells on biogas. *Ionics*, 9(5-6), 336-341.
- [35] Wojcik, A., Middleton, H., Damopoulos, I., & Van Heerle, J. (2003). Ammonia as a fuel in solid oxide fuel cells. *Journal of Power Sources*, 118(1-2), 342-348.
- [36] Murray, E. P., Harris, S. J., & Jen, H. (2002). Solid oxide fuel cells utilizing dimethyl ether fuel. *Journal of Electrochemical Society*, 149(9), A1127-A1131.
- [37] Ahmend, S., Krumpelt, M., Kumar, R., Lee, S. H. D., Carter, J. D., Wilkenhoener, R., & Marshall, C. (1998). Catalytic partial oxidation reforming of hydrocarbon fuels. Technical Report CMT/CP96059, Argonne National Laboratory.
- [38] Simell, P., Kurkela, E., Stahlberg, P., & Hepola, J. (1996). Catalytic hot gas cleaning of gasification gas. *Catalysis Today*, 27, 55-62.
- [39] Ma, L., Verelst, H., & Baron, G.V. (2005). Integrated high temperature gas cleaning: tar removal in biomass gasification with a catalytic filter. *Catalysis Today*, 105, 729-734.

- [40] Leone, P., Lanzini, A., Delhomme, B., Ortigoza-Villalba, G. A., Smeacetto, F., & Santarelli, M. (2012). Analysis of the thermal field of a seal-less planar solid oxide fuel cell. *Journal of Power Sources*, 204, 100-105.
- [41] Morel, B., Roberge, R., Savoie, S., Napporn, T. W., & Meunier, M. (2007). An experimental evaluation of the temperature gradient in solid oxide fuel cells. *Electrochemical and Solid-State Letter*, 10(2), B31-B33.
- [42] Wang, Y., Yoshiba, F., Kawase, M., & Watanabe, T. (2009). Performance and effective kinetic model of methane steam reforming over Ni/YSZ anode of planar SOFC. *International Journal of Hydrogen Energy*, 34, 3885-3893.
- [43] Ivanov, P. (2007). Thermodynamic modeling of the power plant based on the sofc with internal steam reforming of methane. *Electrochimica Acta*, 52(12), 3921-3928.
- [44] Arteaga, L. E., Peralta, L. M., Kafarov, V., Casas, Y., & Gonzales, R. (2008). Bioethanol steam reforming for ecological syngas and electricity production using a fuel cell SOFC system. *Chemical Engineering Journal*, 136(2-3), 256-266.
- [45] Dokmaingama, P. (2010). Modeling of IT-SOFC with indirect internal reforming operation fueled by methane: Effect of oxygen adding as autothermal reforming. *International Journal of Hydrogen Energy*, 35, 13271-13279.
- [46] Dokmaingama, P. (2009). Modeling of SOFC with indirect internal reforming operation: Comparison of conventional packed-bed and catalytic coated-wall internal reformer. *International Journal of Hydrogen Energy*, 34, 410-421.
- [47] Ioraa, P., Aguiarb, P., Adjimanb, C. S., & Brandonb, N. P. (2005). Comparison of two IT DIR-SOFC models: Impact of variable thermodynamic, physical, and flow properties. Steady-state and dynamic analysis. *Chemical Engineering Science*, 60, 2963-2975.
- [48] Churakova, E. M., Badmaev, S. D., Snytnikov, P. V., Gubanov, A. I., Filatov, E. Y., Plyusnin, P. E., Belyaev, V. D., Korenev, S.V., & Sobyenin, V. A. (2010). Bimetallic rhco/zro2 catalysts for ethanol steam conversion into hydrogen-containing gas. *Kinetics and Catalysis*, 51, 893-897.
- [49] Yang, Y., Ma, J., & Wu, F. (2006). Production of hydrogen by steam reforming of ethanol over a ni/zno catalyst. *International Journal of Hydrogen Energy*, 31, 877-882.
- [50] Snytnikov, P. V., Badmaev, S. D., Volkova, G. G., Potemkin, D. I., Zyryanova, M. M., Belyaev, V. D., & Sobyenin, V. A. (2012). Catalysts for hydrogen production in a multifuel processor by methanol, dimethyl ether and bioethanol steam reforming for fuel cell applications. *International Journal of Hydrogen Energy*.
- [51] Sobyenin, V. A., Cavallaro, S., & Freni, S. (2002). Dimethyl ether steam reforming to feed molten carbonate fuel cells (MCFCs). *Energy Fuels*, 14, 1139-1142.
- [52] Fleisch, T. H., Sills, R. A., & Briscoe, M. D. (2002). Emergence of the gas-to liquids industry: a review of global gtl developments. *Journal of Natural Gas Chemistry*, 11, 1-14.

- [53] Kupecki, J., Jewulski, J., & Badyda, K. (2011). Selection of a fuel processing method for SOFC-based micro-CHP system. *Rynek Energii*, 97(6), 157-162.
- [54] Faungnawakij, K., Tanaka, Y., Shimoda, N., Fukunaga, T., Kawashima, S., Kikuchi, R., & Eguchi, K. (2007). Hydrogen production from dimethyl ether steam reforming over composite catalysts of copper ferrite spinel and alumina. *Applied Catalysis B: Environmental*, 74, 144-151.
- [55] Yamada, Y., Mathew, T., Ueda, A., Hiroshi, S., & Tetsuhiko, K. (2006). A novel DME steam-reforming catalyst designed with fact database on demand. *Applied Surface Science*, 252, 2593-2597.
- [56] Tanaka, Y., Kikuchi, R., Takeguchi, T., & Eguchi, K. (2005). Steam reforming of dimethyl ether over composite catalysts of γ -Al₂O₃ and Cu-based spinel. *Applied Catalysis B: Environmental*, 57, 211-222.
- [57] Semelsberger, T. A., Ott, K. C., Borup, R. L., & Greene, H. L. (2006). Generating hydrogen-rich fuel-cell feeds from dimethyl ether (DME) using physical mixtures of a commercial Cu/Zn/Al₂O₃ catalyst and several solid-acid catalysts. *Applied Catalysis A: General*, 65, 291-300.
- [58] Feng, D., Wang, Y., Wang, D., & Wang, J. (2009). Steam reforming of dimethyl ether over CuO-ZnO-Al₂O₃-ZrO₂ + ZSM-5: A kinetic study. *Chemical Engineering Journal*, 146, 477-485.
- [59] Kee, R. J., Korada, P., Walters, K., & Pavol, M. (2002). A generalized model of the flow distribution in channel networks of planar fuel cells. *Journal of Power Sources*, 109(1), 148-159.
- [60] Maharudrayya, S., Jayanti, S., & Deshpande, A. P. (2006). Pressure drop and flow distribution in multiple parallel-channel configurations used in proton-exchange membranes fuel cell stack. *Journal of Power Sources*, 157(1), 358-367.
- [61] Krist, K., & Jewulski, J. (2006). A Radiation-Based Approach to the Design of Planar, Solid Oxide Fuel Cell Modules. *Journal of Materials Engineering and Performance*, 15, 468-473.
- [62] Jewulski, J., Krist, K., Petri, R., & Pondo, J. (2008). Gas Process Panels Integrated with Solid Oxide Fuel Cell Stacks, U.S. Patent No. 7374834.
- [63] Jewulski, J., Blesznowski, M., & Stepien, M. (2009). Flow Distribution Analysis of the Solid Oxide Fuel Cell Stack under Electric Load Conditions, Proceedings of the 9th European SOFC Forum, Lucerne, Switzerland.
- [64] Boersma, R. J., & Sammes, N. M. (1997). Distribution of gas flow in internally manifolded solid oxide fuel-cell stacks. *Journal of Power Sources*, 66, 441-452.
- [65] Alanne, Kari, Saari, Arto, & Ugursal, V. Ismet. (2006). Joel Good The financial viability of an SOFC cogeneration system in single-family dwellings. *Journal of Power Sources*, 158, 403-416.

- [66] Wakui, T., Yokoyama, R., & Shimizu, K. (2010). Suitable operational strategy for power interchange operation using multiple residential SOFC (solid oxide fuel cell) cogeneration systems. *Energy*, 35, 740-750.
- [67] Badwal, S., Deller, R., Foger, K., Ramprakash, Y., & Zhang, J. (1997). Interaction between chromia forming alloy interconnects and air electrode of solid oxide fuel cells. *Solid State Ionics*, 99(3-4), 297-310.
- [68] Andrade, T., & Muccillo, R. (2011). Effect of zinc oxide and boron oxide addition on the properties of yttrium-doped barium zirconate. *Ceramica*, 57(342), 244-253.
- [69] Christman, K., & Jensen, M. (2011). Solid oxide fuel cell performance with cross-flow roughness. *Journal of Fuel Cell Science and Technology*, 2011, 8(2), 024501.1-5.
- [70] Findeisen, W. (1973). *Poradnik inżyniera automatyka*. Wydawnictwa Naukowo-Techniczne.
- [71] Furusaki, A., Konno, H., & Furuichi, R. (1995). Pyrolytic process of la(iii)-cr(vi) precursor for the perovskite type lanthanum chromium oxide. *Thermochimica Acta*, 253, 253-264.
- [72] Hayashi, H., Watanabe, M., & Inaba, H. (2000). Measurement of thermal expansion coefficient of LaCrO_3 . *Thermochimica Acta*, 359(1), 77-85.
- [73] Milewski, J. (2010). Advanced mathematical model of sofc for system optimization. In: ASME Turbo Expo 2010: Power for Land, Sea and Air. No. GT2010-22031. ASME.
- [74] Milewski, J. Advanced model of solid oxide fuel cell. *Fuel Cell Science, Engineering & Technology Conference*. No. FuelCell 2010-33042, ASME.
- [75] Milewski, J. (2010). Mathematical model of SOFC for complex fuel compositions. *International Colloquium on Environmentally Preferred Advanced Power Generation*, ICE-PAG2010-3422.
- [76] Milewski, J. (2010). Simultaneously modelling the influence of thermal-flow and architecture parameters on solid oxide fuel cell voltage. *ASME Fuel Cell Science and Technology*.
- [77] Milewski, J. (2011). SOFC hybrid system optimization using an advanced model of fuel cell. *Proceedings of the 2011 Mechanical Engineering Annual Conference on Sustainable Research and Innovation*, 121-129.
- [78] Milewski, J., Badyda, K., & Miller, A. (2010). Modelling the influence of fuel composition on solid oxide fuel cell by using the advanced mathematical model. *Rynek Energii*, 88(3), 159-163.
- [79] Milewski, J., & Miller, A. (2004). Mathematical model of SOFC (Solid Oxide Fuel Cell) for power plant simulations. *ASME Turbo Expo*, 7, 495-501.
- [80] Milewski, J., Świrski, K., Santarelli, M., & Leone, P. (March 2011). *Advanced Methods of Solid Oxide Fuel Cell Modeling*. 1st Edition, Springer-Verlag London Ltd.

- [81] Sakai, N., & Stolen, S. (1995). Heat capacity and thermodynamic properties of lanthanum(iii) chromate(iii): LaCrO_3 , at temperatures from 298.15 k. evaluation of the thermal conductivity. *The Journal of Chemical Thermodynamics*, 27(5), 493-506.
- [82] Zhai, H., Guan, W., Li, Z., Xu, C., & Wang, W. (2008). Research on performance of LSM coating on interconnect materials for SOFCs. *Journal of the Korean Ceramic Society*, 45(12), 777-781.

IntechOpen

